npj Parkinson's Disease

https://doi.org/10.1038/s41531-026-01271-5

Article in Press

Metagenomics indicates an interplay of the microbiome and functional pathways in Parkinson's disease

Received: 25 July 2025

Accepted: 12 January 2026

Cite this article as: Park, S.J., Özdinç, B.E., Coker, K.G. *et al.* Metagenomics indicates an interplay of the microbiome and functional pathways in Parkinson's disease. *npj Parkinsons Dis.* (2026). https://doi.org/10.1038/s41531-026-01271-5

Sarah Jaehwa Park, Barış Erhan Özdinç, Kathryn Grace Coker, Dana M. Walsh, Devon J. Fox, Samantha Evans, Joshua Farahnik, Kelly Moffat, Margaret Boomgaarden & Laurie K. Mischley

Metagenomics Indicates an Interplay of the Microbiome and Functional Pathways in Parkinson's Disease

Sarah Jaehwa Park[1], Barış Erhan Özdinç[2], Kathryn Grace Coker[1], Dana M Walsh[2], Devon J. Fox[3], Samantha Evans[1], Joshua Farahnik[1], Kelly Moffat[2], Margaret Boomgaarden[1], Laurie K. Mischley[1,3,4*]

1 Bastyr University Research Institute, Bastyr University, Kenmore, WA, USA.

2 CosmosID Inc., Germantown, MD, USA.

3 Parkinson Center for Pragmatic Research, Shoreline, WA, USA.

4 University of Washington, Department of Radiology, Seattle, WA, USA.

[*] **Correspondence:** Laurie K. Mischley, Bastyr University Research Institute, 14500 Juanita Dr NE, Kenmore, WA 98028, Phone: (425) 602-3000, Email: lmischley@bastyr.edu

Running title: Metagenomics and Parkinson's Disease

ABSTRACT

Previous studies suggest there are distinct gut microbial and functional variations in patients with Parkinson's disease (PwPD) that may reveal potential microbiome signatures or biomarkers to aid in early detection of the disease. In this case-control study, we used whole genome sequencing to compare the stool samples of 55 PwPD to 42 healthy controls (HC) from a public database (BioProject Accession PRJEB39223). For bacterial phyla, we observed a greater relative abundance in *Firmicutes* and *Actinobacteria* among PwPD, while that of *Bacteroidetes* was lower. For phages, PwPD had a greater relative abundance of *Siphoviridae, Tectiviridae, and Podoviridae*, while *Microviridae* was lower. Moreover, we described 10 functional pathways that most significantly differed between PwPD and HC (all $P<0.0001$). In conclusion, significant differences were observed in gut bacteria, phages, and functional pathways between PwPD and HC that both support and conflict with previous case-control studies and warrant further validation.

Keywords: Parkinson's disease, gut-brain axis, microbiome, metagenome, whole genome sequencing, gut microbiota, gastrointestinal dysfunction

INTRODUCTION

Parkinson's disease (PD) is a progressive neurodegenerative disease characterized by the loss of nigrostriatal dopaminergic innervation and the aggregation of misfolded α-synuclein (1). Gastrointestinal dysfunction—one of the earliest and most common nonmotor manifestations of PD—often precedes or parallels the onset of motor symptoms (2–4). PD has also been positively associated with several gastrointestinal conditions, including chronic constipation (5,6), irritable bowel syndrome (7,8), inflammatory bowel disease (9), and colonic diverticular disease (10). As such, it has been postulated PD pathophysiology is mediated, in part, through the gut microbiota (11,12). Gut dysbiosis can promote inflammation, intestinal permeability, and aberrant immune responses, all of which have been implicated in α-synuclein misfolding and downstream neurodegenerative processes (11,13,14). Animal studies demonstrate that microbial changes precede motor dysfunction in PD (12,15) and that these shifts are required to induce α-synucleinopathy, neuroinflammation, and motor deficits (13,15). These findings have intensified interest in identifying potential gut microbial signatures or biomarkers for PD.

Whole genome sequencing (WGS) enables a comprehensive analysis of genetic content, including bacteria, viruses, fungi, protists, and functional metabolic pathways. An increasing number of WGS-based observational studies have been conducted in patients with PD (PwPD) in Germany (16), China (17–20), South Korea (21), Taiwan (22,23), Japan (24), Italy (25), London (26), Canada (27,28), and the US (29,30). However, findings have varied across cohorts, and further research is needed to validate these findings. To build on this growing body of work, we

conducted a case-control study using WGS to characterize gut microbial composition and functional pathways in PwPD and healthy controls (HCs) in a North American cohort.

RESULTS

Baseline characteristics for PwPD and HC are presented in **Table 1**. In the PD group, the mean age was 66.0 years, and sex was evenly distributed. Participants were primarily based in the US (95.0%), representing 17 states, and most identified as white (90.9%). Over half reported an annual household income exceeding $150,000 USD (50.9%), and having obtained a graduate or professional degree (50.9%). In terms of clinical characteristics, nearly all participants had idiopathic PD (98.2%), with an average of 7.0 years since diagnosis; over half were classified as Hoehn and Yahr stage 1 (56.4%). In the control group, the mean age was 54.8 years; 76.2% were female; and all were based in Massachusetts, USA.

Bacteria

At the phylum level, PwPD exhibited greater relative abundance of *Firmicutes* and *Actinobacteria* and lower abundance of *Bacteroidetes* and an unclassified phylum compared with HCs (all $P<0.05$; **Figure 1**). PwPD demonstrated significantly higher bacterial α-diversity by both the Shannon (Wilcoxon Rank Sum $P=0.004$; **Figure 2A**) and Simpson indices ($P=0.0002$; **Figure 2B**), reflecting greater community evenness and dominance relative to HCs. In contrast, Chao1 was significantly lower in PwPD ($P<0.0001$; **Figure 2C**), indicating reduced bacterial taxonomic richness. Bray-Curtis β-diversity revealed significant differences in overall community composition between groups (permutational multivariate analysis of variance [PERMANOVA]

P=0.001; **Figure 2D**). While heat map visualization did not demonstrate clear group separation (**Figure S1**), linear discriminant analysis effect size (LEfSe) identified 56 bacterial taxa within the *Firmicutes, Actinobacteria*, *Bacteroidetes*, and unclassified phyla that were differentially enriched between groups (**Figure 3**).

Phages and viruses

Phage community composition differed between PwPD and HC at the family level. On visual inspection of group-level differences, PwPD exhibited lower abundance of *Microviridae* and *Podoviridae* and higher abundance of *Myoviridae*, *Siphoviridae,* and *Tectiviridae* compared with HCs (**Figure S2A**). Phage α-diversity differed between groups, with PwPD demonstrating both greater evenness by Simpson's index (*P*=0.01; **Figure 4A**) and taxonomic richness by Chao1 index (*P*=0.001; **Figure 4B**), while Shannon diversity did not differ significantly (data not shown). Bray-Curtis β-diversity analysis revealed borderline-significant dissimilarity between phage community structure between groups (*P*=0.047; **Figure 4C**). Heat map visualization suggested potential differences in phage family-level relative abundance patterns between PD and HC samples, with some clustering by groups observed, although substantial inter-individual variability was also present (**Figure S2B**).

Bray-Curtis β-diversity analysis of DNA viruses demonstrated significant dissimilarity between PwPD and HCs (**Figure S3**; *P*=0.001). In the heat map (**Figure S4**), we observed some HC samples with relatively high abundance of the *Adenoviridae* but little detection of viral families in PwPD (**Figure S4**).

Protists and fungi

Similar to findings of DNA viruses, Bray-Curtis β-diversity analysis indicated overall compositional differences between PwPD and HCs (*P*=0.001; **Figure S5**). However, visual inspection of the heat map showed low overall abundance of fungal species and high inter-individual variability across samples, resulting in limited statistical power to detect group-level differences (**Figure S6**). In contrast, protist communities did not differ significantly between groups by β-diversity (*P*=0.091; **Figure S7**), indicating broadly similar community composition in PwPD and HCs. Heat map visualization revealed low overall abundance of detected protists and sporadic presence of taxa across samples (**Figure S8**). Nevertheless, *Blastocystis* species were detected more frequently among PwPD than HCs, although this observation was descriptive and not supported by formal statistical testing.

Functional pathways

Lastly, functional profiling revealed marked differences in predicted metabolic potential between PwPD and HC. PwPD demonstrated significantly greater functional α-diversity, with higher Simpson (*P*<0.001; **Figure 5A**) and Chao1 indices (*P*<0.001; **Figure 5B**), indicating both greater evenness and a larger number of detectable MetaCyc pathways. Bray-Curtis β-diversity showed clear separation between groups (*P*=0.001; **Figure 5C**), suggesting distinct functional pathway compositions differences in PwPD. We then examined individual MetaCyc pathway terms that significantly differed in mean abundance between groups. The top 10 most significantly different pathways included: pentose phosphate pathway, fatty acid and β-oxidation I, inosine-5-

phosphate biosynthesis III, anhydromuropeptide recycling, trichloroacetic acid (TCA) cycle VI, colanic acid building blocks biosynthesis, transfer RNA (tRNA) processing, phosphoenolpyruvate carboxykinase (PEPCK)-type C4 photosynthetic carbon assimilation cycle, guanosine nucleotide degradation III, and glutaryl CoA degradation (all $P<0.0001$; **Figure 6**).

DISCUSSION

In this North American case-control study, we observed significant gut microbial and functional differences between PwPD and HC using WGS. PwPD exhibited distinct bacterial community structure characterized by altered phylum-level composition and differences in α- and β-diversities, alongside shifts in the relative abundance of phage families. β-diversity analyses further demonstrated significant differences in overall community composition of phages, viruses, and fungi between PwPD and HCs, suggesting broad multi-kingdom alterations in the gut microbiome associated with PD. Functional profiling also revealed significant differences in predicted microbial metabolic potential, with enrichment of multiple MetaCyc pathways in PwPD.

Firmicutes and *Bacteroidetes* represent the two dominant bacterial phyla in the human gut microbiome, and changes in their composition have been implicated in metabolic and inflammatory conditions (31,32). An increased *Firmicutes* to *Bacteroidetes* (F/B) ratio has been associated with obesity (31,33–35), while a decreased ratio has been reported during weight loss (31) and in inflammatory bowel disease (35–37). Given the increased prevalence of weight loss and gastrointestinal inflammation in PwPD, a reduced F/B ratio might be expected in PD (9,38).

However, our observation of an increased F/B ratio aligns with several prior WGS-based studies (16,17,20,29,30), suggesting this finding may characterize PD-associated gut dysbiosis despite differing clinical phenotypes.

Lower concentrations of fecal short chain fatty acids (SCFAs) have been observed in PwPD (17,39–42) and linked to worse cognitive and motor outcomes compared with HC (17). However, previous studies have reported both a lower (29,30) and greater abundance (43) of SCFA-producing bacteria among PwPD. Although some taxa within the *Firmicutes, Actinobacteria, and Bacteroidetes* phyla include SCFA producers (44), phylum-level shifts do not necessarily reflect changes in specific SCFA-producing taxa. In the present study, we did not observe enrichment of well-characterized SCFA-producing genera and therefore cannot infer altered SCFA production capacity, particularly in the absence of metabolite measurements. Further research integrating fecal and plasma SCFA measurement with metagenomic data is needed to clarify whether changes in microbial composition correspond to alterations in SCFA production and how these may relate to PD outcomes.

We observed notable differences in the phageome between PwPD and HCs, with changes consistent with observations in inflammatory bowel disease (45). Tetz et al (46) reported similar findings and proposed that shifts toward lytic phage populations may reflect dysregulation of bacteriophage-bacteria interactions in PD, potentially contributing to bacterial community instability. However, because phage-host relationships were not examined in the present study, our findings should be interpreted descriptively. Previous PD studies have both supported (16)

and conflicted (17,46) our results for phage α- and β-diversities, and additional work is needed to determine whether phage alterations represent disease-specific signatures or nonspecific features of gut dysbiosis.

Recently, a study from Taiwan (47) also showed that hepatitis C virus infection is associated with PD risk, and the influenza virus, Coxsackie virus, Japanese encephalitis virus, and HIV have also been associated with secondary PD (48,49). In the present study, we identified reduced detection of DNA viral families in PwPD, consistent with findings reported by Bedarf et al (16). In contrast, Qian et al (18) reported viral enrichment in PD and suggested these discrepancies could be due to differences in viral databases and extraction methods. Study location and population may also contribute to differences in virome profiles, as our findings were concordant with German (16) but not Chinese PD cohorts (18). Future studies with harmonized viral reference databases and diverse cohorts are needed to clarify whether virome alterations are consistently associated with PD.

Lastly, we observed significant differences in several functional pathways between PwPD and HC. Current literature and WGS limitations constrain inferences about the pathways identified; however, mechanistic evidence on byproducts of these pathways may suggest linkages to PD pathogenesis. For instance, tRNA processing is disrupted under stress conditions, leading to the accumulation of tRNA-derived fragments (tRFs) (50,51). tRFs have been proposed as potential biomarkers in PD and other neurodegenerative disorders (52–54). Unique tRF signatures have been observed in serum, cerebrospinal fluid, and the prefrontal cortex of PwPD (50,51), but

whether microbiome-associated tRNA processing contributes to peripheral or neuronal tRF pools remains unknown.

The guanosine nucleotide degradation III pathway was also enriched in PwPD. Metcalfe-Roach et al (28) similarly reported perturbations in purine nucleotide metabolism in PD. As degradation of guanine nucleotides contributes to uric acid production acid (55), and lower uric acid levels have been associated with PD risk and progression (56–60), these findings may reflect altered purine metabolism in PwPD. However, whether enrichment of this pathway represents compensatory microbial adaptation or reduced metabolic throughput cannot be determined without corresponding uric acid measurements. Further research is needed to elucidate whether these functional pathways may induce differences in metabolite concentration with linkages to PD symptoms.

Another functional pathway enriched in PwPD was the colanic acid biosynthesis pathway. Colanic acid is a stress-induced exopolysaccharide that promotes bacterial adhesion to the intestinal mucosa and has been associated with mucosal inflammation in conditions such as Crohn's disease (61). Similar enrichment of exopolysaccharide- and capsule-associated pathways has been reported in an independent PD cohort (62), suggesting that microbial cell-envelope stress responses may be a recurring finding across PD metagenomic studies. Although speculative, prior work showing that intestinal inflammation correlates with α-synuclein expression in enteric neurites (63) raises the possibility that such microbial changes may occur within a pro-inflammatory gut environment.

The pentose phosphate pathway was also enriched in PwPD, a finding of interest because this pathway generates nicotinamide adenine dinucleotide phosphate (NADPH), a critical cofactor for antioxidant defense. Dysregulation of the pentose phosphate pathway has been implicated in oxidative stress and neuroinflammation in PD, and its enrichment in the microbiome may reflect bacterial adaptation to increased oxidative stress in the gut microenvironment (64). Finally, we additionally observed differences in pathways related to fatty acid β-oxidation, glutaryl-CoA degradation, anhydromuropeptide recycling, and alternative TCA cycle variants. Although there is limited evidence suggesting their relevance in PD, these pathways may be consistent with microbial metabolic responses to physiological stress, nutrient fluctuations, or other patterns observed in inflammatory gastrointestinal conditions (65,66). Future studies integrating metagenomics with metabolomic and host inflammatory markers will be important for clarifying the biological and clinical significance of these pathways.

This study has several important limitations. First, we used historical controls to characterize our HC group, which introduces the possibility of technical confounding, as samples were processed using different library preparation kits by different people, in different labs, and with different protocols and instruments. These methodological differences can introduce batch effects that influence taxonomic and functional comparisons, making it difficult to determine whether some observed differences reflect true biological variation or differences arising from sample processing. In addition, because the historical controls lacked harmonized sociodemographic, clinical, and lifestyle data, we were unable to adjust for factors that meaningfully shape dietary

habits and the gut microbiota. As a result, our findings warrant further validation and should be considered hypothesis-generating.

Second, potential changes in the concentrations of byproducts or their associations with functional pathways could not be determined, as we did not collect metabolite data. Gene copy number variations also prevented a clear correlation between bacterial abundance and pathway gene expression. As a result, functional pathway differences identified in this study should be interpreted as reflecting predicted metabolic potential rather than actual metabolic activity. Without corresponding metabolomic measurements, we cannot determine whether the observed pathway enrichment results in meaningful shifts in metabolite production, host exposure, or biological relevance to PD. Integrating metagenomics with metabolomic and transcriptomic data in future studies will be critical for validating these pathway-level findings and clarifying their physiological impact. Third, detection of DNA viruses, fungi, and protists was sparse, limiting statistical power and interpretation in these domains. Finally, the PD group was predominantly white, affluent, well-educated, and based in North America, limiting the generalizability of the findings to the broader PD population.

Nevertheless, this case-control study contributes to the growing body of metagenomic research in PD. These findings should be viewed as hypothesis-generating and underscore the need for prospective, multi-omics studies in diverse populations to identify potential microbiome signatures or biomarkers that could enhance the prediction, diagnosis, and treatment of PD.

METHODS

Sample population

This study was conducted according to the guidelines of the Declaration of Helsinki and approved by the Institutional Review Board of Bastyr University (IRB #21-1698; approved 1 December 2021), and informed consent was obtained for all participants. In August 2019, 60 individuals with PD from across the US and Canada attended the Bastyr University Parkinson Summer School, an annual intensive five-day retreat in Washington state. Prior to the retreat, stool sample collection kits were mailed to participants' homes, and 57 participants provided and mailed samples directly to the CosmosID laboratory. Two samples were excluded from analysis because one was from outside of North America and the other arrived more than six months after the others, resulting in a total of 55 PD cases. Data for 42 HCs were obtained from a publicly available dataset (BioProject Accession PRJEB39223; PREDICT1) (67) and were selected to match the PD group by country (US) and age distribution.

Whole genome sequencing

PD stool samples were stored at -80^{o} C until extraction and processed within one month of receipt at the CosmosID laboratory. Microbial DNA from PD samples was extracted using the Qiagen Powersoil Pro Kit. DNA libraries were prepared using the Nextera XT DNA Library Preparation Kit (Illumina) with IDT Unique Dual Indexes (1 ng DNA input) and purified using Ampure magnetic beads (Beckman Coulter). Libraries were quantified using a Qubit 4 fluorometer with the Qubit™ double-stranded DNA High-Sensitivity Assay Kit and sequenced on the Illumina NextSeq 2000 platform with paired-end 150 base-pair reads. As described previously

(67), HC samples were extracted using the Qiagen Dneasy 96 PowerSoil Pro Kit, and DNA libraries were prepared using the NEBNext Ultra II Kit and sequenced on the Illumina NovaSeq 6000 platform.

Taxonomic profiling

Taxonomic classification and relative abundance profiling were performed using the CosmosID-HUB platform, which applies a *k*-mer reference-matching algorithm against curated microbial reference databases. Taxonomic calls were filtered using CosmosID default quality thresholds. Bacterial analyses were conducted using non-subsampled data due to consistently high sequencing depth, whereas viral, phage, fungal, and protist analyses were performed using profiles subsampled to 10 million reads per sample.

Functional profiling

Initial quality control, adapter trimming and preprocessing of metagenomic sequencing reads were done using BBDuk (68). The quality-controlled reads were then subjected to a translated search against a comprehensive and non-redundant protein sequence database, UniRef_90. The UniRef90 database, provided by UniProt (69), represents a clustering of all non-redundant protein sequences in UniProt, such that each sequence in a cluster aligns with 90% identity and 80% coverage of the longest sequence in the cluster. The mapping of metagenomic reads to gene sequences were weighted by mapping quality, coverage, and gene sequence length to estimate community-wide weighted gene family abundances. Gene families were then annotated to MetaCyc (70) reactions (metabolic enzymes) to reconstruct and quantify MetaCyc metabolic

pathways in the community (69). To facilitate comparisons across multiple samples with different sequencing depths, the abundance values were normalized using total-sum scaling normalization to produce “copies per million,” analogous to transcripts per million (TPMs) in RNA sequencing (RNA-Seq) units. Functional pathway profiling was conducted using reads subsampled to 8 million per sample.

Data analyses

Relative abundance stacked bar plots were generated from CosmosID-HUB using phylum-, family-, and species-level filtered matrices. Heat maps were used to visualize cross-sample patterns in relative abundance and clustering of taxa within microbial domains, and were interpreted descriptively. Descriptive observations based on visual inspection of stacked bar plots and heat maps were identified as such and were not treated as quantitative comparisons.

For α-diversity, Shannon, Simpson, and Chao1 indices were visualized in boxplots, and group-level differences were evaluated using Wilcoxon Rank-Sum tests. β-diversity was visualized via principal coordinates analysis (PCoA), with dissimilarity computed using the Bray-Curtis index. Group-level differences were assessed via PERMANOVA. For bacteria, LefSe was calculated based on phylum-, genus-, species-, and strain-level matrices with a Kruskal-Wallis α-value of 0.05, a Wilcoxon α-value of 0.05, and a linear discriminant analysis (LDA) score threshold of 2.0 (71).

For all analyses, *P* values <0.05 were considered statistically significant. *P* values were not adjusted for multiple comparisons, and results were interpreted as hypothesis-generating. All analyses were performed within the CosmosID-HUB comparative analysis module.

ACKNOWLEDGEMENTS

The authors would like to thank the patients who participated in the Bastyr University Parkinson Summer School and provided us with their stool samples. The authors would also like to thank research assistants, Ali DeMatteo and Fjorda Jusufi, for their help with the study.

Author Contributions: LKM, BEO, and DMW contributed to the conception of the study and design of the study. BEO, DMW, and KM performed the statistical analysis, data curation, and data visualization. LKM provided supervision and DJF provided management of the project. LKM, SEE, JF were involved in data collection. SJP and BEO wrote the first draft of the manuscript. All authors: provided critical edits to the manuscript and read and approved the submitted version.

Funding: None declared.

Conflict of Interest: Authors BEO, DMW, KM were employed by CosmosID Inc at the time of the study. The remaining authors declare that the research was conducted in the absence of any commercial or financial relationships that could be construed as a potential conflict of interest.

Data Availability: The datasets generated and/or analyzed during the current study are not publicly available because the processed outputs incorporate proprietary algorithms and reference databases owned by CosmosID but are available from the corresponding author on reasonable request.

Supplementary Material: Figures S1-S8 are provided in a separate document.

REFERENCES

1. Jankovic J. Parkinson's disease: Clinical features and diagnosis. Vol. 79, Journal of Neurology, Neurosurgery and Psychiatry. 2008.
2. Braak H, Braak E. Pathoanatomy of Parkinson's disease. J Neurol. 2000 Apr;247 Suppl 2:II3-10.
3. Cersosimo MG, Raina GB, Pecci C, Pellene A, Calandra CR, Gutiérrez C, et al. Gastrointestinal manifestations in Parkinson's disease: prevalence and occurrence before motor symptoms. J Neurol. 2013 May;260(5):1332–8.
4. Skjærbæk C, Knudsen K, Horsager J, Borghammer P. Gastrointestinal Dysfunction in Parkinson's Disease. J Clin Med. 2021 Jan 31;10(3).
5. Zeng J, Wang X, Pan F, Mao Z. The relationship between Parkinson's disease and gastrointestinal diseases. Front Aging Neurosci. 2022;14:955919.
6. Adams-Carr KL, Bestwick JP, Shribman S, Lees A, Schrag A, Noyce AJ. Constipation preceding Parkinson's disease: a systematic review and meta-analysis. J Neurol Neurosurg Psychiatry. 2016 Jul;87(7):710–6.
7. Lin CH, Lin JW, Liu YC, Chang CH, Wu RM. Risk of Parkinson's disease following severe constipation: a nationwide population-based cohort study. Parkinsonism Relat Disord. 2014 Dec;20(12):1371–5.
8. Lu S, Jiang HY, Shi YD. Association between irritable bowel syndrome and Parkinson's disease: A systematic review and meta-analysis. Acta Neurol Scand. 2022 Apr;145(4):442–8.

9. Zhang X, Svn Z, Liv M, Yang Y, Zeng R, Huang Q, et al. Association Between Irritable Bowel Syndrome and Risk of Parkinson's Disease: A Systematic Review and Meta-Analysis. Front Neurol. 2021;12:720958.

10. Zhu F, Li C, Gong J, Zhu W, Gu L, Li N. The risk of Parkinson's disease in inflammatory bowel disease: A systematic review and meta-analysis. Dig Liver Dis. 2019 Jan;51(1):38–42.

11. Macerollo A, Lu MK, Huang HC, Chen HJ, Lin CC, Kao CH, et al. Colonic diverticular disease: A new risk factor for Parkinson's disease? Parkinsonism Relat Disord. 2017 Sep;42:61–5.

12. Mulak A, Bonaz B. Brain-gut-microbiota axis in Parkinson's disease. World J Gastroenterol. 2015 Oct 7;21(37):10609–20.

13. Liddle RA. Parkinson's disease from the gut. Brain Res. 2018 Aug 15;1693(Pt B):201–6.

14. Sampson TR, Debelius JW, Thron T, Janssen S, Shastri GG, Ilhan ZE, et al. Gut Microbiota Regulate Motor Deficits and Neuroinflammation in a Model of Parkinson's Disease. Cell. 2016 Dec 1;167(6):1469-1480.e12.

15. Sun MF, Shen YQ. Dysbiosis of gut microbiota and microbial metabolites in Parkinson's Disease. Ageing Res Rev. 2018 Aug;45:53–61.

16. Bhattarai Y, Si J, Pu M, Ross OA, McLean PJ, Till L, et al. Role of gut microbiota in regulating gastrointestinal dysfunction and motor symptoms in a mouse model of Parkinson's disease. Gut Microbes. 2021 Jan 1;13(1):1866974.

17. Bedarf JR, Hildebrand F, Coelho LP, Sunagawa S, Bahram M, Goeser F, et al. Functional implications of microbial and viral gut metagenome changes in early stage L-DOPA-naïve Parkinson's disease patients. Genome Med. 2017 Apr 28;9(1):39.

18. Chen SJ, Chen CC, Liao HY, Lin YT, Wu YW, Liou JM, et al. Association of Fecal and Plasma Levels of Short-Chain Fatty Acids With Gut Microbiota and Clinical Severity in Patients With Parkinson Disease. Neurology. 2022 Feb 22;98(8):e848–58.

19. Qian Y, Yang X, Xu S, Huang P, Li B, Du J, et al. Gut metagenomics-derived genes as potential biomarkers of Parkinson's disease. Brain. 2020 Aug 1;143(8):2474–89.

20. Nie S, Jing Z, Wang J, Deng Y, Zhang Y, Ye Z, et al. The link between increased Desulfovibrio and disease severity in Parkinson's disease. Appl Microbiol Biotechnol. 2023 May;107(9):3033–45.

21. Qian Y, Yang X, Xu S, Wu C, Song Y, Qin N, et al. Alteration of the fecal microbiota in Chinese patients with Parkinson's disease. Brain Behav Immun. 2018 May;70:194–202.

22. Jo S, Kang W, Hwang YS, Lee SH, Park KW, Kim MS, et al. Oral and gut dysbiosis leads to functional alterations in Parkinson's disease. NPJ Parkinsons Dis. 2022 Jul 7;8(1):87.

23. Yan Z, Yang F, Cao J, Ding W, Yan S, Shi W, et al. Alterations of gut microbiota and metabolome with Parkinson's disease. Microb Pathog. 2021 Nov;160:105187.

24. Chen SJ, Wu YJ, Chen CC, Wu YW, Liou JM, Wu MS, et al. Plasma metabolites of aromatic amino acids associate with clinical severity and gut microbiota of Parkinson's disease. NPJ Parkinsons Dis. 2023 Dec 14;9(1):165.

25. Nishiwaki H, Ueyama J, Ito M, Hamaguchi T, Takimoto K, Maeda T, et al. Meta-analysis of shotgun sequencing of gut microbiota in Parkinson's disease. NPJ Parkinsons Dis. 2024 May 21;10(1):106.

26. Bolliri C, Fontana A, Cereda E, Barichella M, Cilia R, Ferri V, et al. Gut Microbiota in Monozygotic Twins Discordant for Parkinson's Disease. Ann Neurol. 2022 Oct;92(4):631–6.

27. De Pablo-Fernandez E, Gebeyehu GG, Flain L, Slater R, Frau A, Ijaz UZ, et al. The faecal metabolome and mycobiome in Parkinson's disease. Parkinsonism Relat Disord. 2022 Feb;95:65–9.

28. Cirstea MS, Sundvick K, Golz E, Yu AC, Boutin RCT, Kliger D, et al. The Gut Mycobiome in Parkinson's Disease. J Parkinsons Dis. 2021;11(1):153–8.

29. Metcalfe-Roach A, Cirstea MS, Yu AC, Ramay HR, Coker O, Boroomand S, et al. Metagenomic Analysis Reveals Large-Scale Disruptions of the Gut Microbiome in Parkinson's Disease. Mov Disord. 2024 Oct;39(10):1740–51.

30. Wallen ZD, Demirkan A, Twa G, Cohen G, Dean MN, Standaert DG, et al. Metagenomics of Parkinson's disease implicates the gut microbiome in multiple disease mechanisms. Nat Commun. 2022 Nov 15;13(1):6958.

31. Boktor JC, Sharon G, Verhagen Metman LA, Hall DA, Engen PA, Zreloff Z, et al. Integrated Multi-Cohort Analysis of the Parkinson's Disease Gut Metagenome. Mov Disord. 2023 Mar;38(3):399–409.

32. Ley RE, Turnbaugh PJ, Klein S, Gordon JI. Microbial ecology: human gut microbes associated with obesity. Nature. 2006 Dec 21;444(7122):1022–3.

33. Mariat D, Firmesse O, Levenez F, Guimarães V, Sokol H, Doré J, et al. The Firmicutes/Bacteroidetes ratio of the human microbiota changes with age. BMC Microbiol. 2009 Jun 9;9:123.

34. Koliada A, Syzenko G, Moseiko V, Budovska L, Puchkov K, Perederiy V, et al. Association between body mass index and Firmicutes/Bacteroidetes ratio in an adult Ukrainian population. BMC Microbiol. 2017 May 22;17(1):120.

35. Magne F, Gotteland M, Gauthier L, Zazueta A, Pesoa S, Navarrete P, et al. The Firmicutes/Bacteroidetes Ratio: A Relevant Marker of Gut Dysbiosis in Obese Patients? Nutrients. 2020 May 19;12(5).

36. Stojanov S, Berlec A, Štrukelj B. The Influence of Probiotics on the Firmicutes/Bacteroidetes Ratio in the Treatment of Obesity and Inflammatory Bowel disease. Microorganisms. 2020 Nov 1;8(11).

37. Kostic AD, Xavier RJ, Gevers D. The microbiome in inflammatory bowel disease: current status and the future ahead. Gastroenterology. 2014 May;146(6):1489–99.

38. Stappenbeck TS, Rioux JD, Mizoguchi A, Saitoh T, Huett A, Darfeuille-Michaud A, et al. Crohn disease: a current perspective on genetics, autophagy and immunity. Autophagy. 2011 Apr;7(4):355–74.

39. Chen Z, Li G, Liu J. Autonomic dysfunction in Parkinson's disease: Implications for pathophysiology, diagnosis, and treatment. Neurobiol Dis. 2020 Feb;134:104700.

40. Unger MM, Spiegel J, Dillmann KU, Grundmann D, Philippeit H, Bürmann J, et al. Short chain fatty acids and gut microbiota differ between patients with Parkinson's disease and age-matched controls. Parkinsonism Relat Disord. 2016 Nov;32:66–72.

41. Mulak A. A controversy on the role of short-chain fatty acids in the pathogenesis of Parkinson's disease. Mov Disord. 2018 Mar;33(3):398–401.

42. Tan AH, Chong CW, Lim SY, Yap IKS, Teh CSJ, Loke MF, et al. Gut Microbial Ecosystem in Parkinson Disease: New Clinicobiological Insights from Multi-Omics. Ann Neurol. 2021 Mar;89(3):546–59.

43. Aho VTE, Houser MC, Pereira PAB, Chang J, Rudi K, Paulin L, et al. Relationships of gut microbiota, short-chain fatty acids, inflammation, and the gut barrier in Parkinson's disease. Mol Neurodegener. 2021 Feb 8;16(1):6.

44. Mao L, Zhang Y, Tian J, Sang M, Zhang G, Zhou Y, et al. Cross-Sectional Study on the Gut Microbiome of Parkinson's Disease Patients in Central China. Front Microbiol. 2021;12:728479.

45. Binda C, Lopetuso LR, Rizzatti G, Gibiino G, Cennamo V, Gasbarrini A. Actinobacteria: A relevant minority for the maintenance of gut homeostasis. Dig Liver Dis. 2018 May;50(5):421–8.

46. Manrique P, Bolduc B, Walk ST, van der Oost J, de Vos WM, Young MJ. Healthy human gut phageome. Proc Natl Acad Sci U S A. 2016 Sep 13;113(37):10400–5.

47. Tetz G, Brown SM, Hao Y, Tetz V. Parkinson's disease and bacteriophages as its overlooked contributors. Sci Rep. 2018 Jul 17;8(1):10812.

48. Tsai HH, Liou HH, Muo CH, Lee CZ, Yen RF, Kao CH. Hepatitis C virus infection as a risk factor for Parkinson disease: A nationwide cohort study. Neurology. 2016 Mar 1;86(9):840–6.

49. Leta V, Urso D, Batzu L, Lau YH, Mathew D, Boura I, et al. Viruses, parkinsonism and Parkinson's disease: the past, present and future. J Neural Transm (Vienna). 2022 Sep;129(9):1119–32.

50. Jang H, Boltz DA, Webster RG, Smeyne RJ. Viral parkinsonism. Biochim Biophys Acta. 2009 Jul;1792(7):714–21.

51. Prehn JHM, Jirström E. Angiogenin and tRNA fragments in Parkinson's disease and neurodegeneration. Acta Pharmacol Sin. 2020 Apr;41(4):442–6.

52. Yu X, Xie Y, Zhang S, Song X, Xiao B, Yan Z. tRNA-derived fragments: Mechanisms underlying their regulation of gene expression and potential applications as therapeutic targets in cancers and virus infections. Theranostics. 2021;11(1):461–9.

53. Magee R, Londin E, Rigoutsos I. TRNA-derived fragments as sex-dependent circulating candidate biomarkers for Parkinson's disease. Parkinsonism Relat Disord. 2019 Aug;65:203–9.

54. Tian H, Hu Z, Wang C. The Therapeutic Potential of tRNA-derived Small RNAs in Neurodegenerative Disorders. Aging Dis. 2022 Apr;13(2):389–401.

55. Kuo MC, Liu SCH, Hsu YF, Wu RM. The role of noncoding RNAs in Parkinson's disease: biomarkers and associations with pathogenic pathways. J Biomed Sci. 2021 Nov 18;28(1):78.

56. Paganoni S, Schwarzschild MA. Urate as a Marker of Risk and Progression of Neurodegenerative Disease. Neurotherapeutics. 2017 Jan;14(1):148–53.

57. Aerqin Q, Jia SS, Shen XN, Li Q, Chen KL, Ou YN, et al. Serum Uric Acid Levels in Neurodegenerative Disorders: A Cross-Sectional Study. J Alzheimers Dis. 2022;90(2):761–73.

58. Seifar F, Dinasarapu AR, Jinnah HA. Uric Acid in Parkinson's Disease: What Is the Connection? Mov Disord. 2022 Nov;37(11):2173–83.

59. Dănău A, Dumitrescu L, Lefter A, Popescu BO. Serum Uric Acid Levels in Parkinson's Disease: A Cross-Sectional Electronic Medical Record Database Study from a Tertiary Referral Centre in Romania. Medicina (Kaunas). 2022 Feb 6;58(2).

60. Shi X, Zheng J, Ma J, Wang Z, Sun W, Li M, et al. Low serum uric acid levels are associated with the nonmotor symptoms and brain gray matter volume in Parkinson's disease. Neurol Sci. 2022 Mar;43(3):1747–54.

61. Ari BC, Tur EK, Domac FM, Kenangil GO. Uric acid: The role in the pathophysiology and the prediction in the diagnosis of Parkinson's disease: A Turkish-based study. Ideggyogy Sz. 2022 Jan 30;75(1–02):51–9.

62. Sartor B. Intestinal bacterial biofilms modulate mucosal immune responses. J Immunol Sci. 2018;2(2).

63. Metcalfe-Roach A, Cirstea MS, Yu AC, Ramay HR, Coker O, Boroomand S, et al. Metagenomic Analysis Reveals Large-Scale Disruptions of the Gut Microbiome in Parkinson's Disease. Movement Disorders. 2024 Oct 28;39(10):1740–51.

64. Stolzenberg E, Berry D, Yang D, Lee EY, Kroemer A, Kaufman S, et al. A Role for Neuronal Alpha-Synuclein in Gastrointestinal Immunity. J Innate Immun. 2017;9(5).

65. Christodoulou D, Kuehne A, Estermann A, Fuhrer T, Lang P, Sauer U. Reserve Flux Capacity in the Pentose Phosphate Pathway by NADPH Binding Is Conserved across Kingdoms. iScience. 2019;19.

66. De Vos WM, Tilg H, Van Hul M, Cani PD. Gut microbiome and health: mechanistic insights. Gut. 2022;71(5).

67. Hou J, Xiang J, Li D, Liu X, Pan W. Gut microbial response to host metabolic phenotypes. Vol. 9, Frontiers in Nutrition. 2022.

68. Asnicar F, Berry SE, Valdes AM, Nguyen LH, Piccinno G, Drew DA, et al. Microbiome connections with host metabolism and habitual diet from 1,098 deeply phenotyped individuals. Nat Med. 2021 Feb;27(2):321–32.

69. Bushnell B. DOE Joint Genome Institute. 2021. BBDuk Guide - DOE Joint Genome Institute.

70. Franzosa EA, McIver LJ, Rahnavard G, Thompson LR, Schirmer M, Weingart G, et al. Species-level functional profiling of metagenomes and metatranscriptomes. Nat Methods. 2018 Nov;15(11):962–8.

71. Caspi R, Billington R, Ferrer L, Foerster H, Fulcher CA, Keseler IM, et al. The MetaCyc database of metabolic pathways and enzymes and the BioCyc collection of pathway/genome databases. Nucleic Acids Res. 2016 Jan 4;44(D1):D471-80.

72. Segata N, Izard J, Waldron L, Gevers D, Miropolsky L, Garrett WS, et al. Metagenomic biomarker discovery and explanation. Genome Biol. 2011;12(6).

FIGURE LEGEND

Figure 1. Phylum-level bacterial community composition in patients with Parkinson's disease and healthy controls.

A Stacked bar plot comparing mean relative abundance of gut bacterial phyla between groups. **B-E** Boxplots comparing relative abundance of *Firmicutes* (B), *Actinobacteria* (C), *Bacteroidetes* (D), and unidentified phyla (E) between groups (all $P<0.05$). Boxes indicate the median and interquartile range; points represent outliers. *P* value was calculated using Wilcoxon rank sum tests. Data are based on non-subsampled bacterial profiles generated using the CosmosID-HUB platform.

Figure 2. Bacterial α- and β-diversities in patients with Parkinson's disease and healthy controls.

A-C Boxplots comparing Shannon (A), Simpson (B), and Chao1 (C) α-diversity indices between groups. Boxes indicate the median and interquartile range; points represent outliers. *P* values were calculated using Wilcoxon rank sum tests. **D** Principal coordinates analysis (PCoA) plot of Bray-Curtis β-diversity. Each point represents an individual subject, with Parkinson's disease samples shown in green and healthy controls in blue. Distances between points reflect differences in phage community composition based on Bray-Curtis dissimilarity. Percent variance explained by each principal coordinate is shown on the axes. *P* value was calculated via PERMANOVA. Data are based on non-subsampled bacterial profiles generated using the CosmosID-HUB platform.

Figure 3. Differentially abundant bacteria in patients with Parkinson's disease and healthy controls.

Cladogram generated using linear discriminant analysis effect size (LEfSe) depicting bacterial taxa significantly enriched in patients with Parkinson's disease (green) or healthy controls (red), organized by phylogenetic hierarchy from phylum to genus. LefSe was calculated with a Kruskal-Wallis α-value of 0.05, a Wilcoxon α-value of 0.05, and a linear discriminant analysis (LDA) score threshold of 2.0. Data are based on non-subsampled bacterial profiles generated using the CosmosID-HUB platform.

Figure 4. Phage α- and β-diversities in patients with Parkinson's disease and healthy controls.

A-B Boxplots comparing Shannon (A) and Chao1 (B) α-diversity indices between groups. Boxes indicate the median and interquartile range; points represent outliers. *P* values were calculated using Wilcoxon rank sum tests. **C** Principal coordinates analysis (PCoA) plot of Bray-Curtis β-diversity. Each point represents an individual subject, with Parkinson's disease samples shown in green and healthy controls in blue. Distances between points reflect differences in phage community composition based on Bray-Curtis dissimilarity. Percent variance explained by each principal coordinate is shown on the axes. *P* value was calculated via PERMANOVA. Data are based on subsampled phage profiling at a depth of 10 million reads per sample using the CosmosID-HUB platform.

Figure 5. Functional pathway α- and β-diversities in patients with Parkinson's disease and healthy controls.

A-B Boxplots comparing Shannon (A) and Chao1 (B) α-diversity indices between groups. Boxes indicate the median and interquartile range; points represent outliers. *P* values were calculated using Wilcoxon rank sum tests. **C** Principal coordinates analysis (PCoA) plot of Bray-Curtis β-diversity. Each point represents an individual subject, with Parkinson's disease samples shown in green and healthy controls in blue. Distances between points reflect differences in functional pathways based on Bray-Curtis dissimilarity. Percent variance explained by each principal coordinate is shown on the axes. *P* value was calculated via PERMANOVA. Data are based on subsampled functional profiling at a depth of 8 million reads per sample using the CosmosID-HUB platform.

Figure 6. Functional pathways enriched in patients with Parkinson's disease.

A-J Boxplots of top 10 MetaCyc pathway terms that had significantly greater mean abundance in patients with Parkinson's disease compared to healthy controls, including pentose phosphate pathway (A), fatty acid and β-oxidation I (B), inosine-5-phosphate biosynthesis III (C), anhydromuropeptides recycling (D), trichloroacetic acid (TCA) cycle VI (E), colanic acid building blocks biosynthesis (F), transfer RNA (tRNA) processing (G), PEPCK-type C4 photosynthetic carbon assimilation cycle (H), guanosine nucleotide degradation III (I), and glutaryl CoA degradation (J). Boxes indicate the median and interquartile range; points represent outliers. *P* values were calculated using Wilcoxon rank sum tests. Data are based on

subsampled functional profiling at a depth of 8 million reads per sample using the CosmosID-HUB platform.

Table 1. Sociodemographic and clinical characteristics of patients with Parkinson's disease compared to healthy controls.[1]

	Parkinson's disease (*n*=55)	Healthy controls (*n*=42)
Age, years – mean ± SD	66 ± 7.7	54.8 (±5.2)
Sex – no. (%)		
Male	27 (45.7%)	10 (23.8%)
Female	28 (54.2%)	32 (76.2%)
Geolocation – no. (%)		
United States	52 (95.0%)	42 (100.0%)
Canada	3 (5.0%)	0 (0.0%)
Race – no. (%)		N/A
White	50 (90.9%)	
Non-white	5 (9.1%)	
Annual household income, USD – no. (%)		N/A
< $60,000	8 (14.5%)	
$60,000 to < $80,000	4 (7.2%)	
$80,000 to < $100,000	7 (12.7%)	
$100,000 to $150,000	6 (10.9%)	
≥ $150,000	30 (50.9%)	
Education level – no. (%)		N/A
Less than college degree	13 (23.6%)	
College degree	14 (25.5%)	
Graduate/professional degree	28 (50.9%)	
Type of Parkinsonism – no. (%)		N/A
Idiopathic Parkinson's disease	54 (98.2%)	
Other Parkinsonism	1 (1.8%)	
Years since Parkinson diagnosis – mean ± SD	7.0 ± 11.5	N/A
Estimated Hoehn & Yahr stage – no. (%)		N/A
1 (unilateral involvement only, minimal disability)	31 (56.4%)	
2 (both sides affected, balance is stable)	13 (23.6%)	
3 (mild to moderate disability, balance affected)	11 (20.0%)	

[1] Data for healthy controls were obtained from a public database (BioProject Accession PRJEB39223). Available sociodemographic information was limited. Clinical characteristics related to Parkinsonism were not applicable.

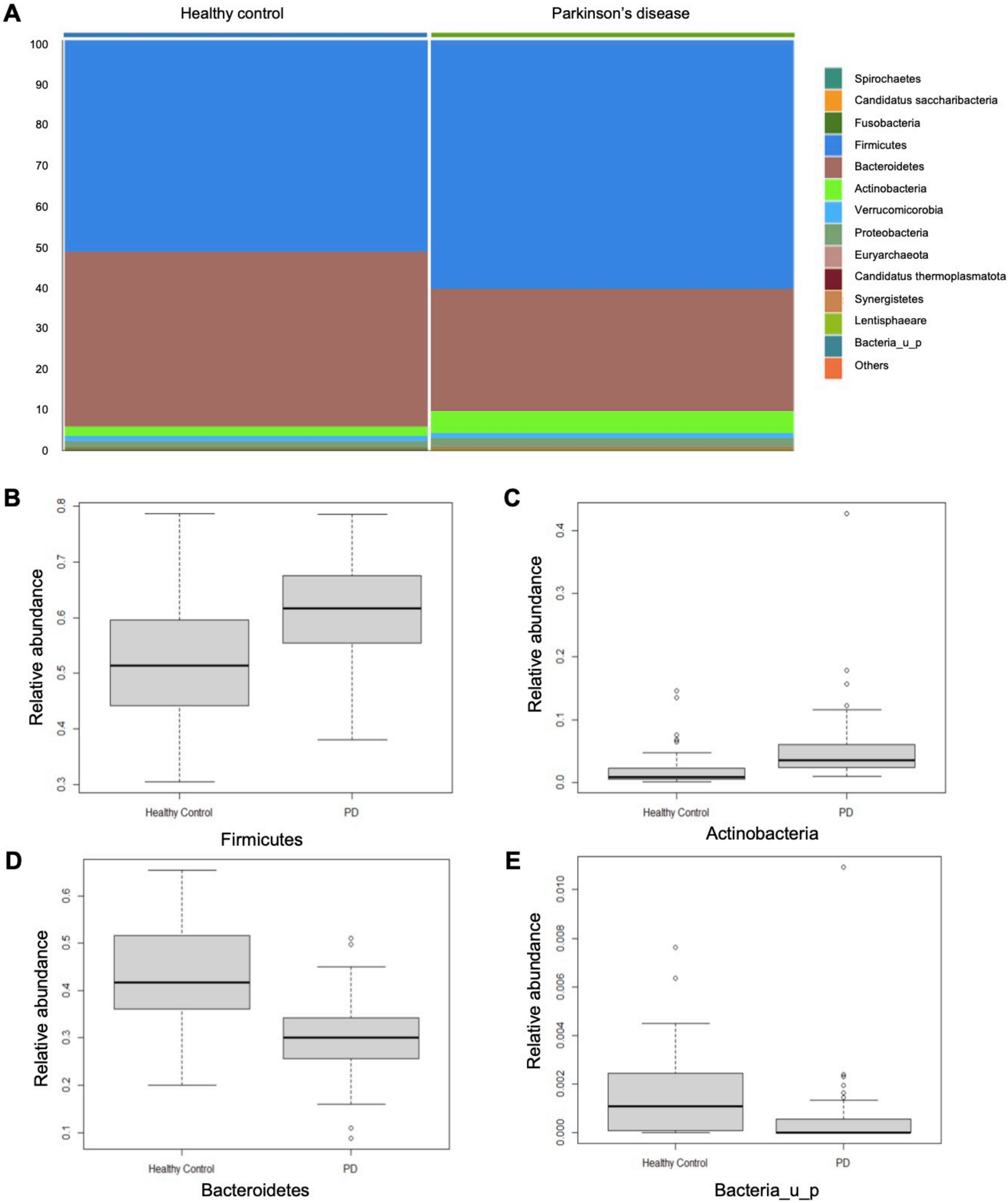
A
Healthy control
Parkinson's disease
100
90
80
70
60
50
40
30
20
10
0
Spirochaetes
Candidatus saccharibacteria
Fusobacteria
Firmicutes
Bacteroidetes
Actinobacteria
Verrucomicorobia
Proteobacteria
Euryarchaeota
Candidatus thermoplasmatota
Synergistetes
Lentisphaeare
Bacteria_u_p
Others
B
Relative abundance
0.8
0.7
0.6
0.5
0.4
0.3
Healthy Control
PD
Firmicutes
C
Relative abundance
0.4
0.3
0.2
0.1
0.0
Healthy Control
PD
Actinobacteria
D
Relative abundance
0.6
0.5
0.4
0.3
0.2
0.1
Healthy Control
PD
Bacteroidetes
E
Relative abundance
0.010
0.008
0.006
0.004
0.002
0.000
Healthy Control
PD
Bacteria_u_p

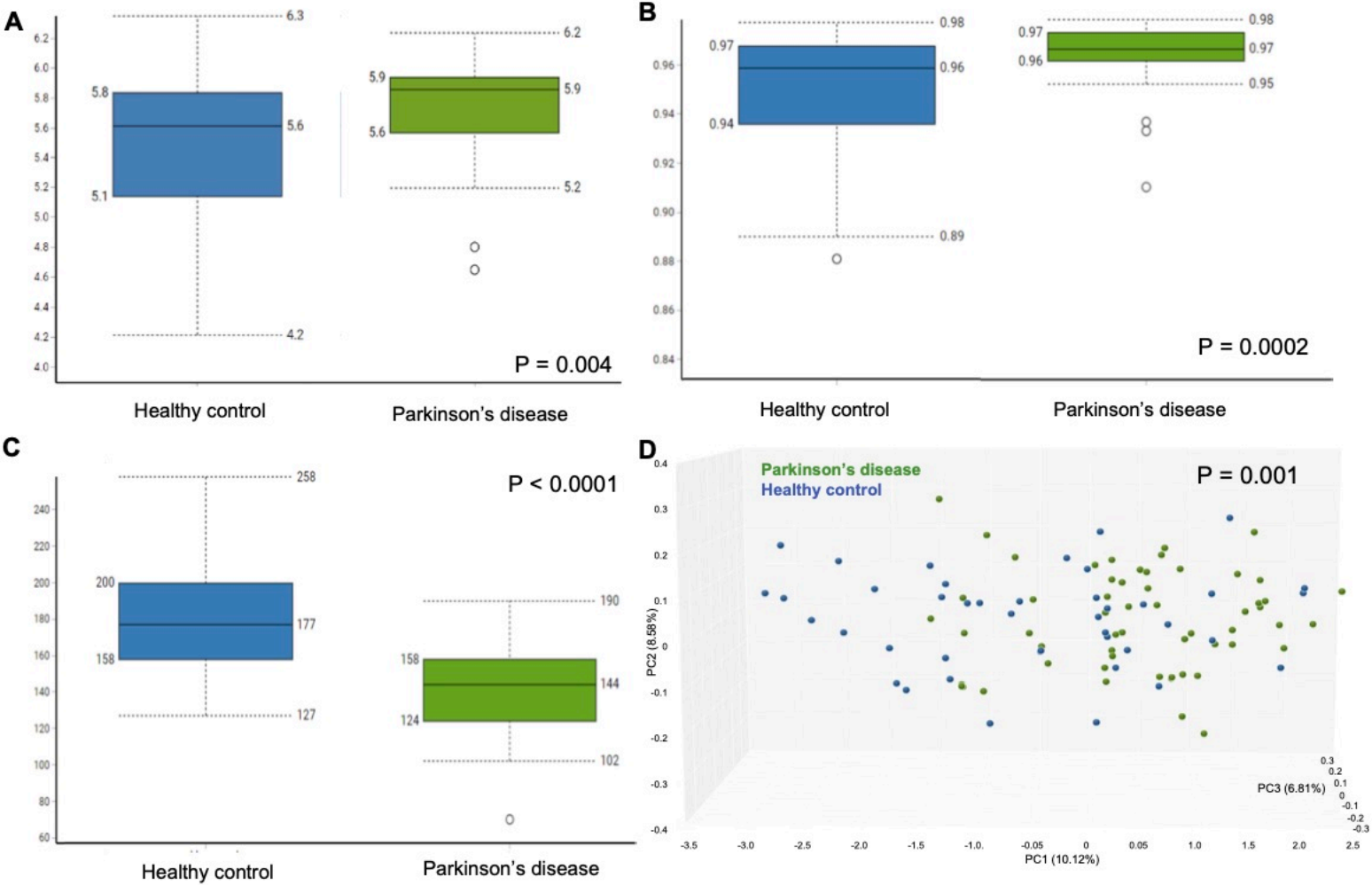
A
6.3
6.2
5.8
5.6
5.1
4.2
5.9
5.6
6.2
5.9
5.2
P = 0.004
Healthy control
Parkinson's disease
B
0.98
0.97
0.96
0.94
0.89
0.98
0.97
0.96
0.97
0.95
P = 0.0002
Healthy control
Parkinson's disease
C
258
200
177
158
127
190
158
144
124
102
P < 0.0001
Healthy control
Parkinson's disease
D
Parkinson's disease
Healthy control
P = 0.001
PC2 (8.58%)
PC3 (6.81%)
PC1 (10.12%)

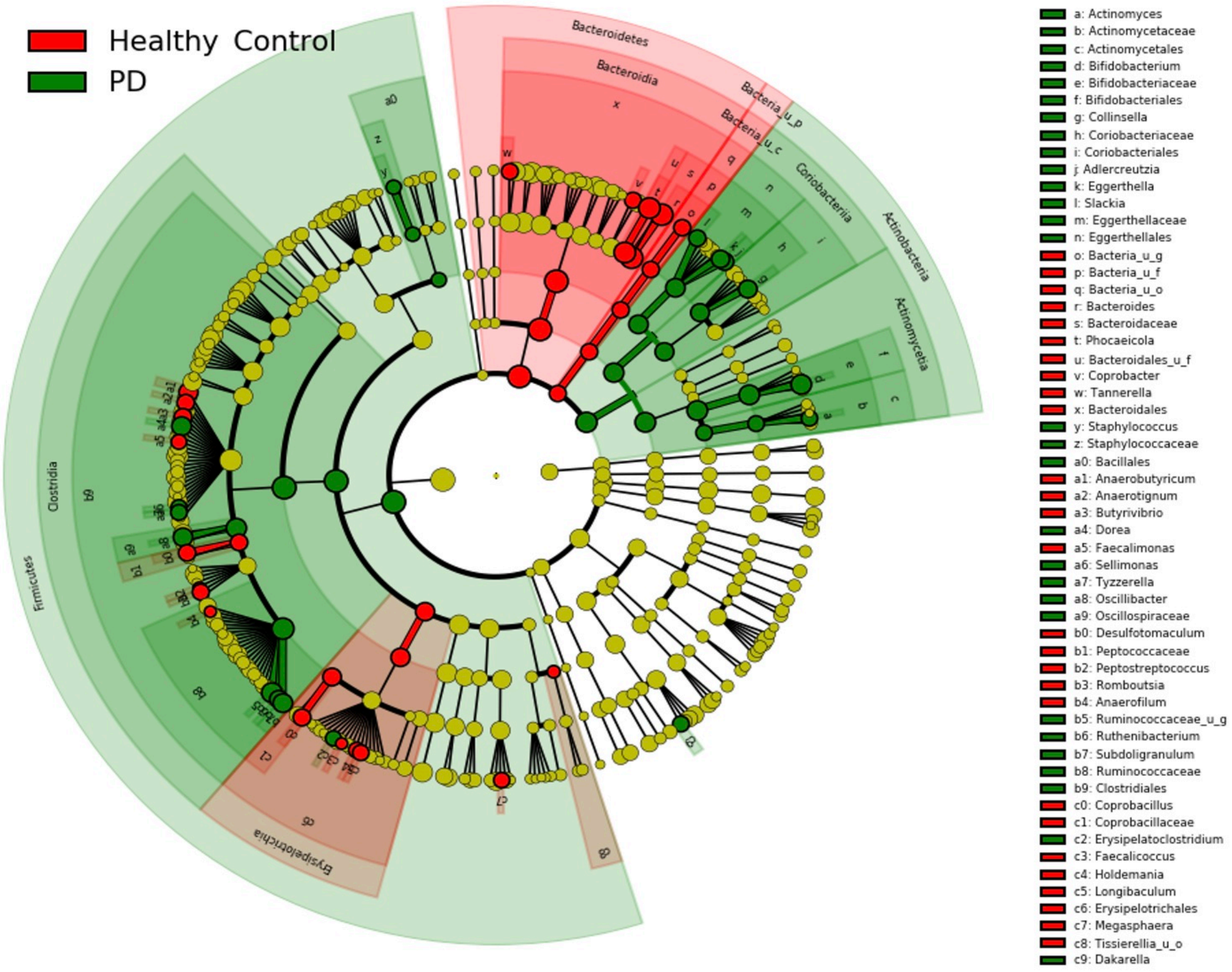
Healthy Control
PD
Bacteroidetes
Bacteroidia
Bacteria_u_p
Bacteria_u_c
Coriobacteriia
Actinobacteria
Actinomycetia
Firmicutes
Clostridia
Erysipelotrichia
a: Actinomyces
b: Actinomycetaceae
c: Actinomycetales
d: Bifidobacterium
e: Bifidobacteriaceae
f: Bifidobacteriales
g: Collinsella
h: Coriobacteriaceae
i: Coriobacteriales
j: Adlercreutzia
k: Eggerthella
l: Slackia
m: Eggerthellaceae
n: Eggerthellales
o: Bacteria_u_g
p: Bacteria_u_f
q: Bacteria_u_o
r: Bacteroides
s: Bacteroidaceae
t: Phocaeicola
u: Bacteroidales_u_f
v: Coprobacter
w: Tannerella
x: Bacteroidales
y: Staphylococcus
z: Staphylococcaceae
a0: Bacillales
a1: Anaerobutyricum
a2: Anaerotignum
a3: Butyrivibrio
a4: Dorea
a5: Faecalimonas
a6: Sellimonas
a7: Tyzzerella
a8: Oscillibacter
a9: Oscillospiraceae
b0: Desulfotomaculum
b1: Peptococcaceae
b2: Peptostreptococcus
b3: Romboutsia
b4: Anaerofilum
b5: Ruminococcaceae_u_g
b6: Ruthenibacterium
b7: Subdoligranulum
b8: Ruminococcaceae
b9: Clostridiales
c0: Coprobacillus
c1: Coprobacillaceae
c2: Erysipelatoclostridium
c3: Faecalicoccus
c4: Holdemania
c5: Longibaculum
c6: Erysipelotrichales
c7: Megasphaera
c8: Tissierellia_u_o
c9: Dakarella

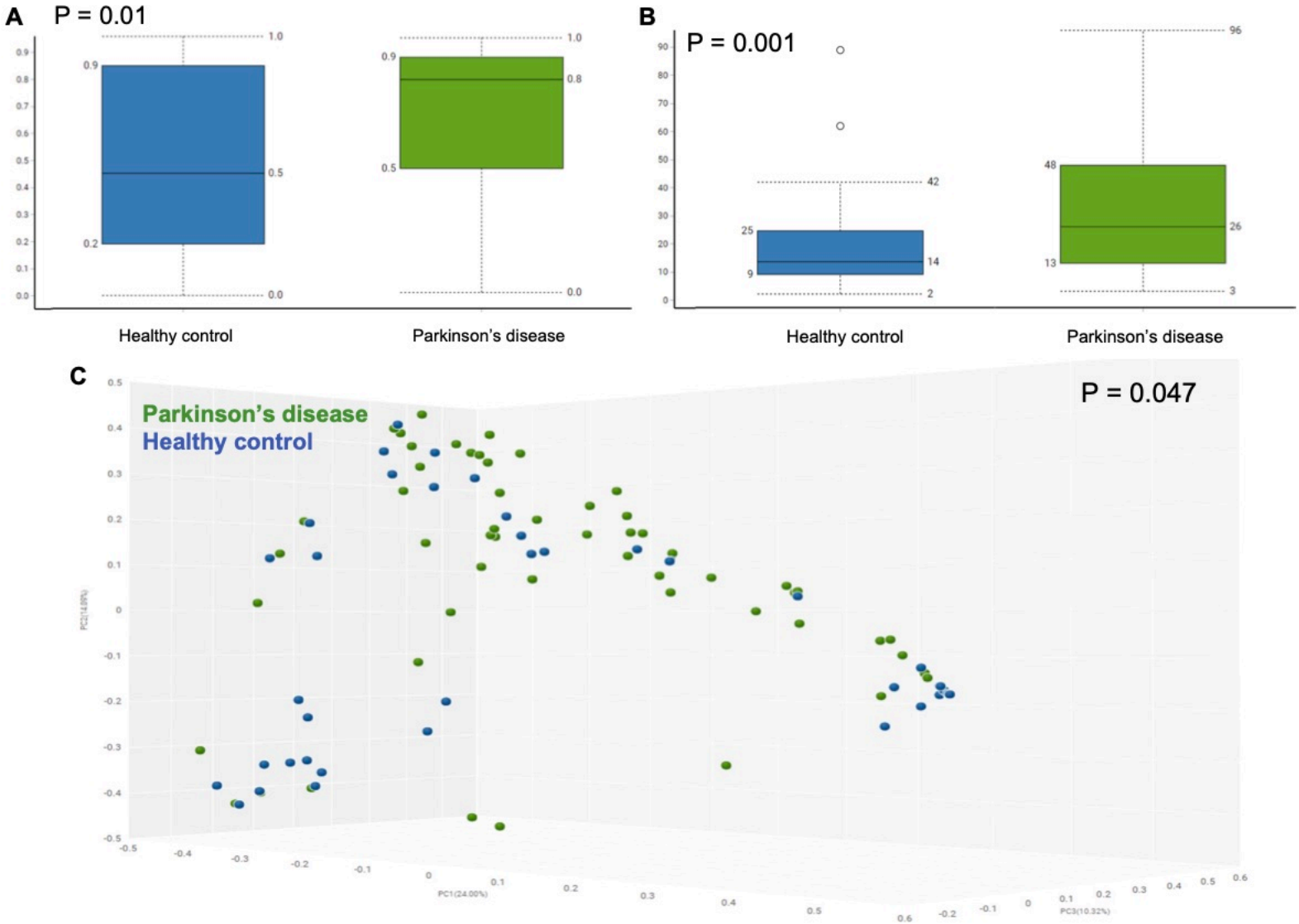
A
P = 0.01
Healthy control
Parkinson's disease
B
P = 0.001
Healthy control
Parkinson's disease
C
Parkinson's disease
Healthy control
P = 0.047
PC1(24.00%)
PC3(10.32%)

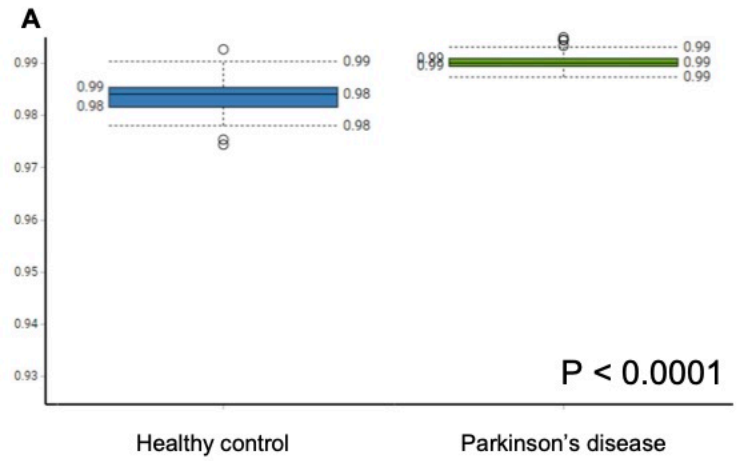
A
0.99
0.98
0.97
0.96
0.95
0.94
0.93
0.99
0.98
0.98
0.99
0.99
0.99
0.99
P < 0.0001
Healthy control
Parkinson's disease

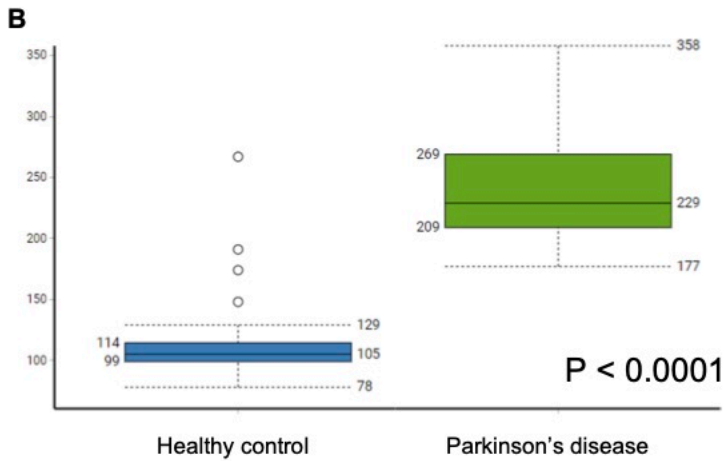
B
350
300
250
200
150
100
129
114
99
105
78
358
269
229
209
177
P < 0.0001
Healthy control
Parkinson's disease

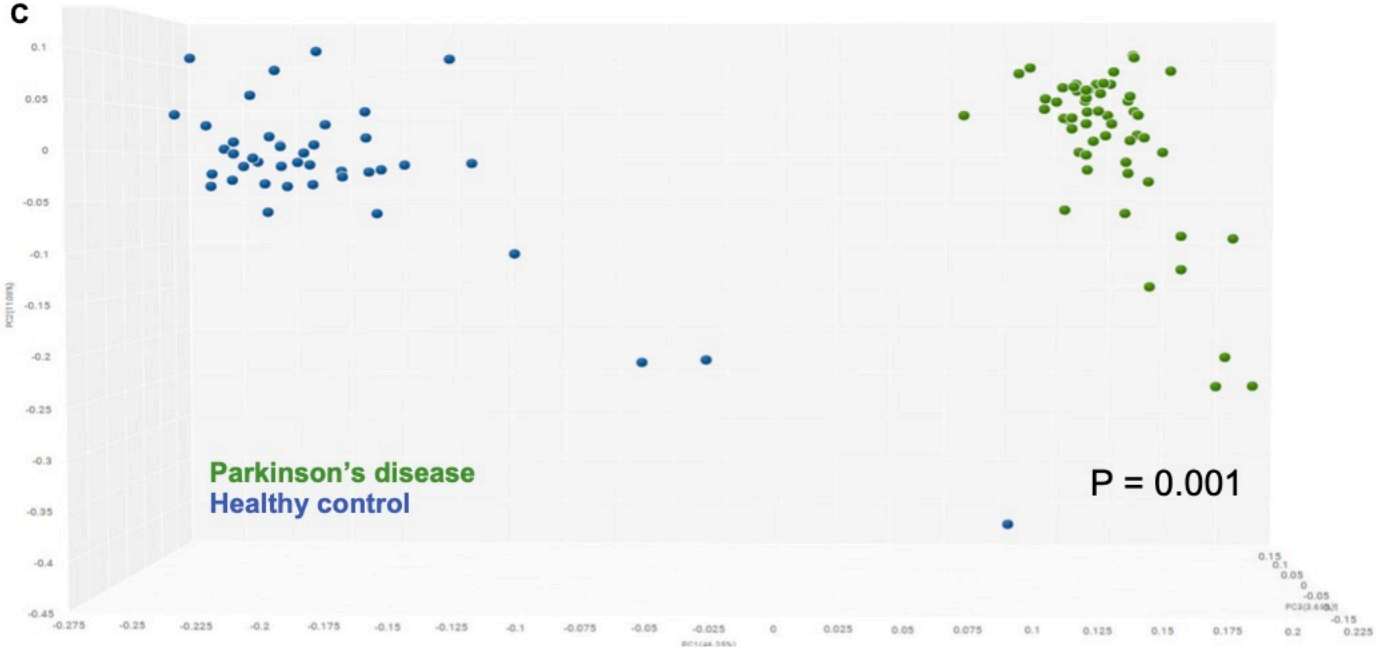
C
Parkinson's disease
Healthy control
P = 0.001

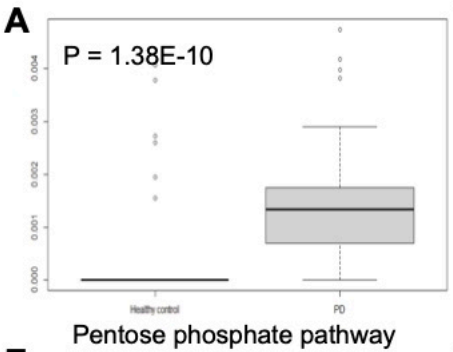

Pentose phosphate pathway

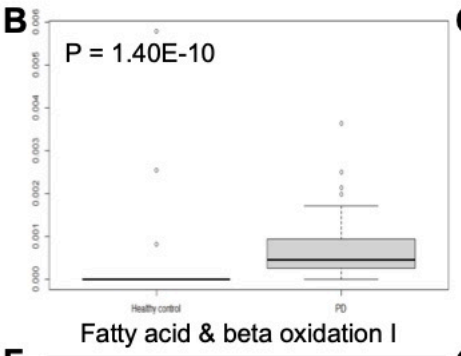

Fatty acid & beta oxidation I

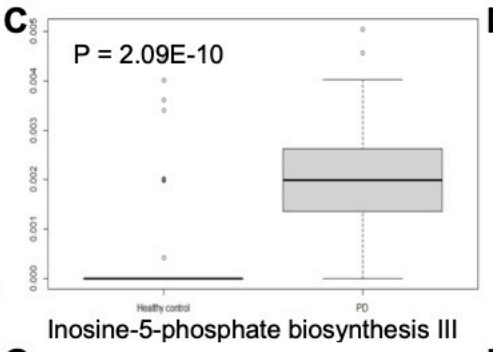

Inosine-5-phosphate biosynthesis III

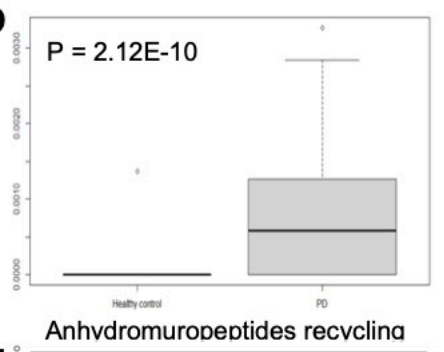

Anhydromuropeptides recycling

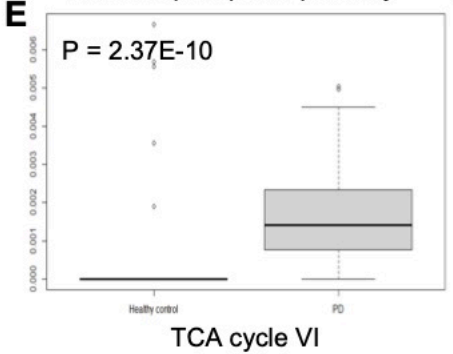

TCA cycle VI
(obligate autotrophs)

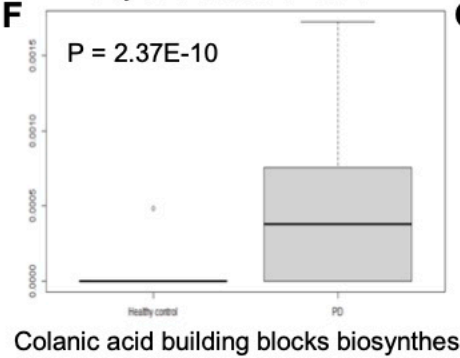

Colanic acid building blocks biosynthesis

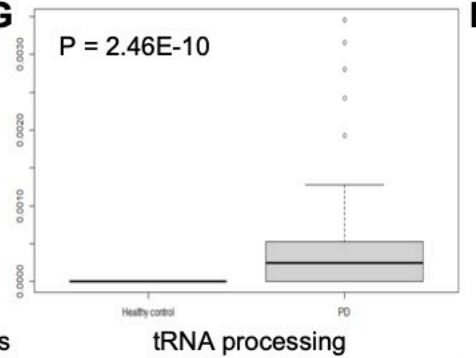

tRNA processing

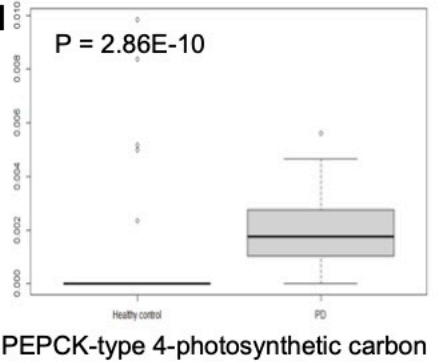

PEPCK-type 4-photosynthetic carbon assimilation cycle

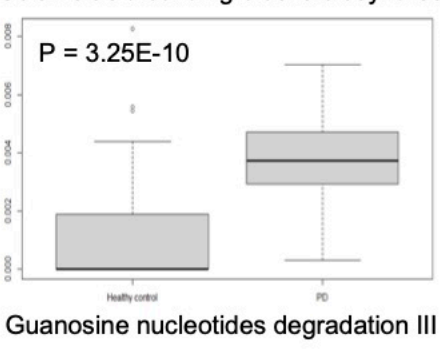

Guanosine nucleotides degradation III

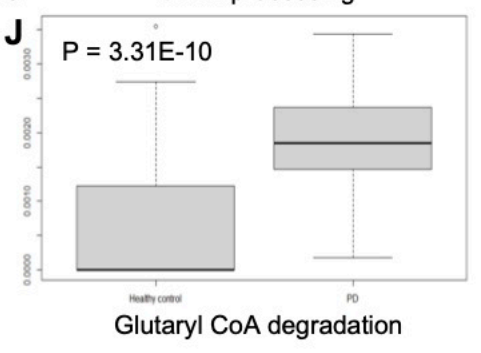

Glutaryl CoA degradation